Malays. J. Anal. Sci. Volume 29 Number 2 (2025): 807

MALAYSIAN JOURNAL OF ANALYTICAL SCIENCES

Journal homepage: https://mjas.analis.com.my/

Research Article

Determination of mercury in cosmetic creams via chitosan-stabilized silver nanoparticle-assisted spectrophotometry

Hendri Wasito[1,2*], Astriana Dian Wahdani[2], and Dadan Hermawan[3]

[1]Department of Pharmacy, Faculty of Health Sciences, Jenderal Soedirman University, Purwokerto, Indonesia.
[2]Analytical Chemistry for Pharmaceutical and Health Research Group, Department of Pharmacy, Jenderal Soedirman University, Purwokerto, Indonesia.
[3]Department of Chemistry, Faculty of Mathematics and Natural Sciences, Jenderal Soedirman University, Purwokerto, Indonesia.

[*]Corresponding author: hendri.wasito@unsoed.ac.id

Received: 1 April 2023; Revised: 28 March 2025; Accepted: 15 April 2025; Published: 24 April 2025

Abstract

Mercury, a toxic heavy metal, continues to be illicitly added to skin-lightening cosmetics despite global bans, posing severe health risks. This study aimed to develop an accurate and rapid method for mercury detection in cosmetic creams using chitosan-stabilized silver nanoparticles (CS-AgNPs). The method leverages Hg^{2+}-induced discoloration of CS-AgNPs, validated for linearity, accuracy, precision, the limit of detection (LOD), and the limit of quantification (LOQ). Synthesized CS-AgNPs exhibited a characteristic surface plasmon resonance (SPR) peak at 420 nm, with an average particle size of 207 nm. The assay demonstrated excellent linearity ($R^2 > 0.97$) across 20-100 µg mL^{-1} Hg^{2+}, with recoveries of 95-101%, and precision (RSD <5%). Detection and quantification limits were 3.6 µg mL^{-1} (LOD) and 12.01 µg mL^{-1} (LOQ), respectively. Based on the experimental findings, CS-AgNPs demonstrate high selectivity and promise for routine mercury analysis in cream samples, exhibiting suitable analytical performance for their intended purpose.

Keywords: Chitosan-stabilized silver nanoparticles, colorimetric detection, cosmetic safety, mercury determination

Introduction

Skin-lightening cosmetics remain widely used by individuals seeking a brighter complexion or reduced facial hyperpigmentation [1]. These products often target melanin, a pigment synthesized in melanosomes, transported to keratinocyte borders via the dendritic process, and subsequently stored in perinuclear regions of keratinocytes and melanocytes [1]. Although mercury-containing cosmetic creams can inhibit melanin synthesis, mercury is a highly toxic element with severe health implications. Even minimal exposure may adversely affect the brain, kidneys, heart, stomach, and intestines [1]. Consequently, mercury is strictly prohibited in cosmetic formulations. Despite regulatory bans, mercury continues to be illicitly added to cosmetic products, posing significant public health risks [2].

Several analytical techniques have been utilized to determine mercury levels, including atomic absorption spectrophotometry (AAS) [3], inductively coupled plasma-mass spectrometry (ICP-MS) [4], high-performance liquid chromatography inductively coupled plasma mass spectrometry (HPLC-ICP-MS) [5], and electrochemical sensor [6]. However, these methods face limitations, including time-intensive procedures, high operational costs, and the requirement for sophisticated instrumentation. In contrast, colorimetry has emerged as a straightforward alternative for mercury detection in cosmetics. This method offers several advantages, such as simplicity, rapid analysis, cost-effectiveness, and user-friendly instrumentation [7]. Recent advances in nanotechnology further enhance this approach, as nanoparticles (NPs) with sub-1 µm dimensions exhibit unique optical properties exploitable for colorimetric sensing [8].

Over recent decades, colorimetric sensors based on silver nanoparticles (AgNPs) and gold nanoparticles (AuNPs) have emerged as promising analytical tools for diverse applications [9]. Although AuNPs are

recognized as the most stable metal nanoparticle, AgNPs of comparable size demonstrate enhanced visibility and sensitivity due to their superior plasmon excitation efficiency [8]. Furthermore, AgNPs are more cost-effective than AuNPs, making them a preferred choice for colorimetric methodologies [8]. AgNPs have been extensively utilized for detecting ions—including iron, copper, lead, cobalt, manganese, mercury—and diverse metabolites [8,10].

Various methods have been developed for synthesizing silver nanoparticles, including chemical reduction [11], electrochemical synthesis [12], photochemical synthesis [13], microemulsion techniques [14], gamma irradiation [15], UV-assisted synthesis [16], microwave-assisted synthesis [17], and green synthesis [18]. However, AgNPs are prone to aggregation, necessitating stabilization strategies to retain their functional properties. Immobilizing nanoparticles within a biopolymer matrix has gained attention enhancing stability. This approach not only increases the active surface area of nanoparticles but also mitigates aggregation, thereby improving their functional performance [19]. Chitosan, a biopolymer composed of β-(1→4)-linked glucosamine and *N*-acetyl-D-glucosamine, stands out as a promising matrix due to its biodegradability, biocompatibility, and non-toxic nature. The presence of amine (-NH_2) and hydroxyl (-OH) functional groups in its structure enables chitosan to act as an effective chelating agent. Under acidic conditions, the protonation of free amine groups facilitates chelation with metal ions through electrostatic interactions, further enhancing its utility in nanoparticle stabilization [20].

To the best our knowledge, no prior studies have reported using chitosan-stabilized silver nanoparticles (CS-AgNPs) in colorimetric methods for detecting mercury in cosmetic products. This study aims to develop a simple, robust, and cost-effective colorimetric approach for mercury detection in cosmetic creams, leveraging the unique advantages of CS-AgNPs. We rigorously validate the analytical performance of this method through systematic spectrophotometric analysis, emphasizing its selectivity, linearity, accuracy, precision, and limits of detection (LOD) and quantification (LOQ) for routine quality control.

Materials and Methods

Chemicals

Analytical-grade silver nitrate ($AgNO_3$), ascorbic acid ($C_6H_8O_6$), and glacial acetic acid (CH_3COOH) were purchased from Merck (Darmstadt, Germany). The chitosan standard was obtained from Sigma Aldrich (St. Louis, USA). Standard solutions of mercury ($Hg(NO_3)_2$), lead ($Pb(NO_3)_2$), cadmium ($Cd(NO_3)_2$), arsenic (H_3AsO_4), and chromium ($Cr(NO_3)_3$) in 2% HNO_3 (1000 μg mL^{-1}) were purchased from Merck (Darmstadt, Germany). High-purity demineralized water was supplied by Bratachem (Purwokerto, Indonesia). Commercially available cosmetic creams were purchased from a local market (Purwokerto, Indonesia).

Instrumentation

Magnetic heated stirrer HMS-79 (Shanghai, China), analytical balance Ohaus (Nänikon, Switzerland), and micropipettes Socorex (Lausanne, Switzerland) were used for CS-AgNPs preparation. The colorimetric measurements were performed with a Cecil CE 3021 UV-Visible spectrophotometer (Cambridge, England), while particle characterization was performed using an SZ-100 Horiba Scientific (Kyoto, Japan) particle size analyzer.

Synthesis and characterization of chitosan-stabilized silver nanoparticles (CS-AgNPs)

The synthesis of CS-AgNPs was adapted from Zain et al. [21] with optimization of key parameters such as chitosan concentrations, silver nitrate ($AgNO_3$) concentration, ascorbic acid concentration, and incubation time. In the optimized procedure, 50 mL of a 1.0 mg mL^{-1} $AgNO_3$ solution was mixed with chitosan dissolved in 1% (v/v) glacial acetic acid. To this mixture, 2.0 mL of 0.5 mg mL^{-1} ascorbic acid was added. The mixed solutions were stirred and incubated at 600 rpm and 90°C for 15 minutes. The resulting CS-AgNPs were stored in the refrigerator at 4°C and in the dark. Characterizations included a UV-Vis spectrophotometer and a particle size analyzer (PSA).

Determination and method validation of mercury using CS-AgNPs

For mercury detection in the samples, 300 μL of sample solutions was mixed with 2.4 mL of CS-AgNPs solutions, followed by adding 3.0 mL of deionized water. The resulting mixture were then incubated at 90°C for 30 minutes. Finally, absorbance measurements were performed at 420 nm (λ_{max}) using a UV-Vis spectrophotometer, with deionized water as the blank. A calibration curve was constructed by plotting mercury concentration against the relative discoloration intensity ($\Delta A = A_0 - A_s$), where A_0 and A_s represent the absorbance of the blank and sample, respectively.

Analytical method validation followed ICH Q2 (R1) guidelines [22], assessing selectivity, linearity, accuracy, precision, and the limits of detection (LOD) and quantification (LOQ). Selectivity was evaluated against 100 μg mL^{-1} solutions of Pb^{2+},

Cd^{2+}, As^{5+}, and Cr^{3+}. Linearity was verified using triplicate measurements of five mercury standards (20-100 μg mL^{-1}). Accuracy was determined via the standard addition method, in which three spiked mercury concentrations were added to the sample solution. For the sample solution, 100 mg of cosmetic cream was dissolved in 50 mL of deionized water and filtered through a 0.22 μm nylon membrane before analysis. All measurements were conducted in triplicate.

Precision was evaluated as intra-day and inter-day variability. Intra-day precision involved three replicate measurements of the same sample within a single day, while inter-day precision extended measurements across three consecutive days, with relative standard deviation (RSD) thresholds set at ≤3% and ≤5%, respectively. LOD and LOQ were derived from the calibration curve using the equations LOD = 3.3 σ/S and LOQ = 10σ/S, where σ represents the residual standard deviation of the regression line, and S denotes its slope.

Results and Discussion

Synthesis and characteristics of chitosan-stabilized silver nanoparticles (CS-AgNPs)

The chitosan-stabilized silver nanoparticles (CS-AgNPs) were synthesized through a chemical reduction method involving silver nitrate, ascorbic acid, and chitosan. During synthesis, adding chitosan dissolved in acetic acid to the $AgNO_3$ solution facilitated electrostatic interactions between Ag^+ ions and the biopolymer's functional groups. Specifically, the amine ($-NH_2$) and hydroxyl (-OH) groups of chitosan—abundant in oxygen and nitrogen atoms—acted as electron donors, interacting with the positively charged silver ions to form Ag^+-chitosan complexes. Ascorbic acid served as a reducing agent to reduce silver ions and facilitate the formation of silver nanoparticles [23]. Additionally, protonated chitosan stabilized the silver nanoparticles, preventing nanoparticle aggregation and controlling their size distribution [21].

Adding ascorbic acid to the silver nitrate and chitosan solutions induced a distinct color transition from bright yellow to a deep yellowish-brown, with the UV-Vis absorption peak at 420 nm (**Figure 1A**). This chromatic shift due to the reduction of Ag+ ions to zerovalent silver nanoparticles (Ag^0), as confirmed by the characteristic surface plasmon resonance (SPR) band in the 400-500 nm range—a characteristic of AgNP formation [10, 19, 23]. The observed SPR peak intensity and position are directly influenced by nanoparticle size and dispersion; larger particles or aggregates exhibit redshifted peaks due to altered plasmonic coupling [8]. Moreover, the absence of chitosan in an acidic ascorbic acid solution leads to unstable AgNPs, as the lack of protonated amine groups ($-NH_3^+$) from chitosan diminished electrostatic stabilization. This underscores the critical role of pH-dependent electrostatic repulsion between anions (e.g., NO_3^-) and the positively charged chitosan matrix in stabilizing AgNPs [24]. Particle size analysis revealed CS-AgNP clusters with an average size of 207 nm (**Figure 1B**), aligned with prior reports of chitosan-mediated AgNP aggregates ranging from 10-500 nm [25].

Optimization of chitosan-stabilized silver nanoparticles (CS-AgNPs) synthesis conditions

This study systematically optimized four critical synthesizing CS-AgNPs: ascorbic acid concentration, silver nitrate ($AgNO_3$) concentration, chitosan concentration, and incubation time. The goal was to establish conditions yielding stable, optically uniform CS-AgNPs. Clear colloidal solutions were

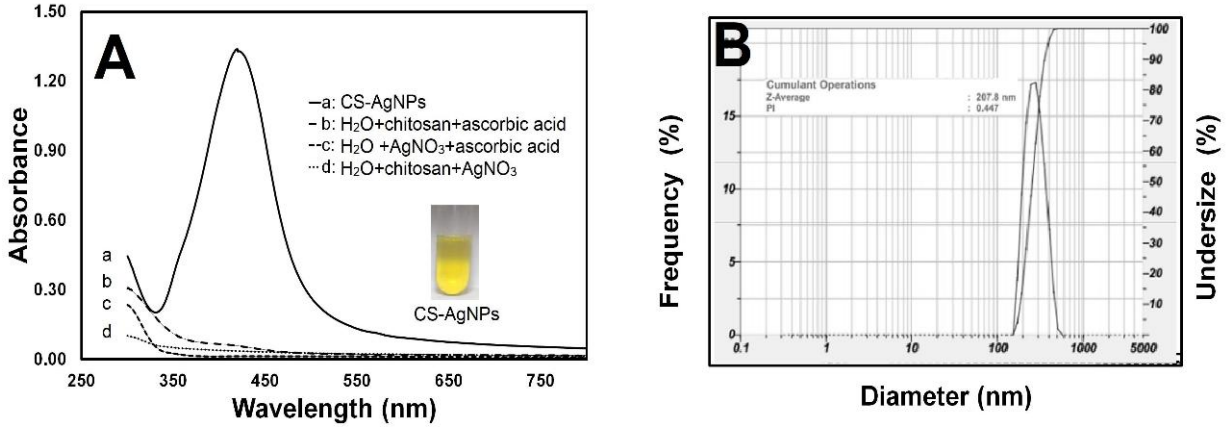

Figure 1. Characterization of chitosan-stabilized silver nanoparticles (CS-AgNPs). (A) UV-Vis absorption spectra of CS-AgNPs and precursor reagents (ascorbic acid, $AgNO_3$, and chitosan). (B) Hydrodynamic size distribution of CS-AgNPs determined by particle size analyzers

prioritized to minimize light scattering artifacts during spectrophotometric measurements, as turbid suspensions can artificially inflate absorbance values.

The first step in this process involved selecting the concentration of ascorbic acid by adding varying concentrations of ascorbic acid to a fixed concentration of 1.0 mg mL^{-1} of silver nitrate and chitosan. Absorbance at 420 nm increased with ascorbic acid concentration, suggesting enhanced nanoparticle formation (**Figure 2A**). However, at 0.8 mg mL^{-1}, the solutions appeared a dark yellow with suspended particles, indicating nanoparticle instability due to oversaturation of the reducing agent. This aligns with a prior study that excess ascorbic acid disrupts colloidal stability by promoting rapid, uncontrolled nanoparticle growth and aggregation [23]. Consequently, 0.5 mg mL^{-1} ascorbic acid was selected as the optimal concentration for further investigation.

Reactions were performed with varying $AgNO_3$ concentrations (0.5-2.0 mg mL-1) alongside fixed concentrations of chitosan (1.0 mg mL^{-1}) and ascorbic acid (0.5 mg mL^{-1}). The results showed that absorbance at 420 nm increased proportionally with $AgNO_3$ concentration, correlating with intensified yellowish coloration due to enhanced nanoparticle formation (**Figure 2B**). However, at 2.0 mg mL^{-1} $AgNO_3$, the solution became turbid, indicating aggregation of silver nanoparticles into larger clusters—a phenomenon consistent with prior reports of oversaturated precursor conditions [26]. Therefore, 1.0 mg mL^{-1} $AgNO_3$ was selected for subsequent experiments.

Optimal chitosan concentration was evaluated by varying its concentration (0.1-5.0 mg mL^{-1}) in reactions containing 0.5 mg mL^{-1} ascorbic acid and 1.0 mg mL^{-1} $AgNO_3$. Adding 1.0 mg mL^{-1} chitosan and 0.5 mg mL^{-1} ascorbic acid was sufficient to reduce silver nitrate at a concentration of 1.0 mg mL^{-1} (**Figure 2C**). Chitosan serves not only as a stabilizing agent but also as a reducing agent in the synthesis of silver nanoparticles [27].

The synthesis mixture (1.0 mg mL^{-1} $AgNO_3$, 0.5 mg mL^{-1} ascorbic acid, 1.0 mg mL^{-1} chitosan) was stirred and heated at 90℃ for 15-60 minutes. Absorbance at 420 nm increased with incubation time (**Figure 2D**), peaking at 30 and 60 minutes with a distinct yellow hue indicative of well-dispersed nanoparticles. This finding corroborates other observations suggesting that synthesizing silver nanoparticles with a stirring time exceeding 30 minutes can lead to a darker yellowish hue due to increased particle collisions, ultimately resulting in aggregation [28]. Thus, 15 minutes was an optimal duration to ensure monodisperse CS-AgNPs.

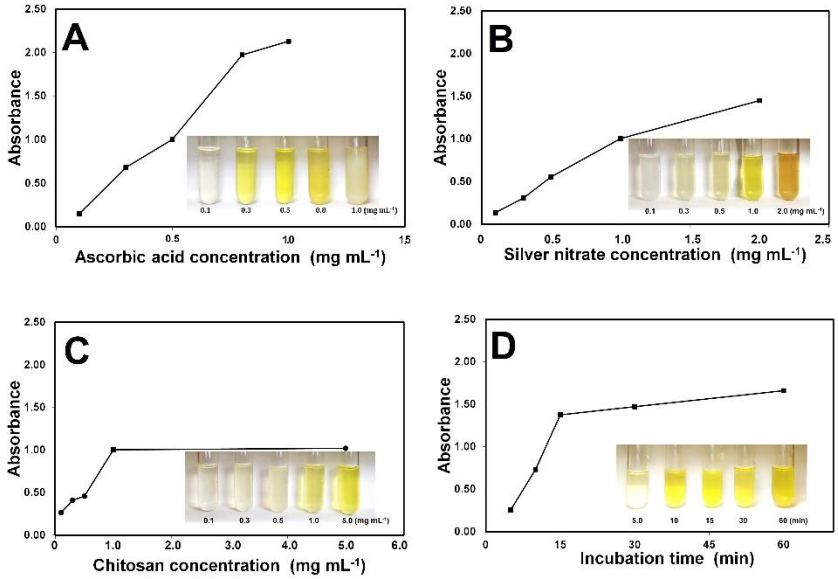

Figure 2. Optimization of chitosan-stabilized silver nanoparticles (CS-AgNPs) synthesis. Effect of varying concentrations of (A) ascorbic acid, (B) silver nitrate ($AgNO_3$), and (C) chitosan, as well as (D) incubation time, on nanoparticle synthesis.

Determination and method validation of mercury using CS-AgNPs

The selectivity of the CS-AgNPs-based colorimetric method was evaluated by incubating synthesized nanoparticles with solutions containing Hg^{2+} and common interferent ions (Pb^{2+}, Cd^{2+}, As^{5+}, Cr^{3+}) at 90 °C for 15 minutes. A pronounced decrease in absorbance at 420 nm—corresponding to SPR attenuation—was observed exclusively with Hg^{2+}, while other ions induced negligible spectral changes (**Figure 3A**), indicating that the method demonstrated high selectivity for mercury (Hg^{2+}) over other metal ions. This finding aligns with previous studies demonstrating Hg^{2+}-specific redox interactions with AgNPs. The mechanism involves the oxidation of zerovalent silver atoms (Ag^0) in AgNPs to Ag^+ ions, coupled with the reduction of Hg^{2+} to elemental mercury (Hg^0), as confirmed by UV-Vis spectroscopy and transmission electron microscopy (TEM) analysis. Conversely, SPR showed only a small shift following the addition of various metal ion solutions, including Al^{3+}, As^{3+}, As^{5+}, Cd^{2+}, Co^{2+}, Cr^{+6}, Cu^{2+}, Fe^{2+}, Fe^{3+}, and Pb^{2+} [29].

The sensitivity of the method was demonstrated by incubating CS-AgNPs with Hg^{2+} concentrations ranging from 20–100 µg mL^{-1}. A concentration-dependent decrease in absorbance at 420 nm was observed (**Figure 3B**), accompanied by visible decolorization from yellow to colorless, consistent with Hg^{2+}-mediated nanoparticles. The linear correlation between Hg^{2+} concentration and relative discoloration intensity ($\Delta A = A_0 - A_s$) yielded a calibration curve with a correlation coefficient (R^2) >0.97 (**Figure 3C**).

Accuracy and precision were evaluated using the standard addition method by spiking cosmetic cream samples with mercury at three concentration levels: 75%, 100%, and 125% of the target value. Triplicate measurements were performed for each spiked level (**Table 1**). Accuracy, expressed as percentage recovery, yielded values ranging from 95.66% to 101.06%, demonstrating excellent agreement between measured and added mercury concentrations. These recoveries surpass those reported in other studies, such as 64-88% for mercury determination in cosmetic creams using AAS [3] and >94% using the cold vapor-AAS method [30].

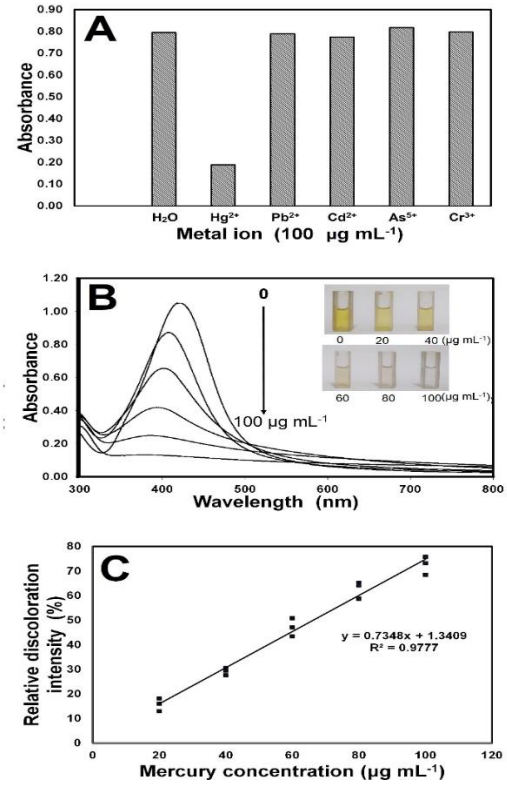

Figure 3. Selectivity and linearity performance of mercury determination. (A) The effect of mercury and other metal ions in CS-AgNPs solutions. (B) UV–Vis spectral changes of CS-AgNPs solutions upon Hg^{2+}-induced aggregation at concentrations ranging from 20-100 µg mL^{-1}. (C) Linear calibration curve in the range of 20-100 µg mL^{-1}

The precision of the measurement, expressed as relative standard deviation (RSD), yielded intraday and interday values of <2% and <5%, respectively (**Table 1**). These results surpass the intraday precision (RSD <7%) reported for mercury determination in cosmetics using AAS [3]. The LOD and LOQ, calculated from the calibration curve's residual standard deviation, were determined as 3.60 µg mL⁻¹ and 12.01 µg mL⁻¹, respectively. Although these values are higher than those achieved by advanced techniques such as ICP-MS [4, 31], the proposed method remains effective for detecting mercury in cosmetics illegally adulterated with concentrations exceeding 1000 µg mL⁻¹ [2]. **Table 2** compares the analytical performance of this method with existing techniques, including cold vapor-AAS, isotope dilution-ICP-MS, and differential pulse stripping voltammetry.

Table 1. Accuracy and precision data for mercury determination (n = 3)

Spike Level	Sample	Mercury Added	Intraday		Interday	
			Mercury Found	Recovery	Mercury Found	Recovery
		(µg mL^{-1})	(µg mL^{-1})	(%)	(µg mL^{-1})	(%)
75%	1	60.00	60.35	100.59	58.01	96.68
	2	60.00	61.31	102.19	60.35	100.59
	3	60.00	60.24	100.40	63.27	105.45
	Average			**101.06**		**100.91**
	% RSD			**0.97**		**4.35**
100%	1	80.00	81.52	101.91	82.90	103.65
	2	80.00	78.42	98.02	77.83	97.29
	3	80.00	79.49	99.35	78.42	98.02
	Average			**99.76**		**99.65**
	%RSD			**1.98**		**3.49**
125%	1	100.00	97.31	97.31	96.74	96.74
	2	100.00	96.65	96.65	96.05	96.05
	3	100.00	93.03	93.03	97.31	97.31
	Average			**95.66**		**96.70**
	% RSD			**2.31**		**0.63**

Table 2. Comparison of analytical method for mercury determination in cosmetic

Sample	Method	Linier range and (R^2)	LOD	Recovery (%)	Intraday RSD (%)	Interday RSD (%)	Ref.
Cosmetic	CV-AAS[a]	0.01–0.04 ppm (0.9984)	0.005 ppm	98-102	2.8 (n=10)	-	[31]
Cosmetic	ID-ICP-MS[b]	Up to 8.0 ng mL^{-1} (0.997)	0.6 pg mL^{-1}	90-105	2.3 (n=7)	5.1 (n=7)	[4]
Cosmetic	AAS[c]	0.05-2.0 µg L^{-1} (>0.99)	0.4749 ng g^{-1}	78.65	12.69 (n=10)	7.17 (n=10)	[3]
Cosmetic	DPSV[d]	10–500 µg L^{-1} (0.993)	5 µg L^{-1}	78.5-107.9	8.8 (n=20)	-	[6]
Cosmetics	CS-AgNPs colorimetry	20 – 100 µg mL^{-1} (0.9777)	3.60 µg mL^{-1}	95.66 - 101.06	0.97 – 2.31 (n=3)	0.63 – 4.35 (n=3)	This work

[a]Cold vapor technique coupled with atomic absorption spectrometry (AAS); [b]Isotope dilution inductively coupled plasma mass spectrometry; [c]Atomic absorption spectrometry; [d]Differential pulse stripping voltammetry;A dash (-) indicates no data available

Conclusion

Our results demonstrate that chitosan-stabilized silver nanoparticles (CS-AgNPs) were effectively developed for detecting mercury in creams using a spectrophotometric method based on discoloration. The proposed method exhibited strong analytical performance, including good linearity, accuracy, and precision, making it highly suitable for analyzing mercury in cosmetic creams.

Acknowledgment

This study was supported by the Institutional Research Program of Jenderal Soedirman University, Puwokerto, Indonesia.

References

1. Pollock, S., Taylor, S., Oyerinde, O., Nurmohamed, S., Dlova, N., Sarkar, R., Galadari, H., Manela-Azulay, M., Chung, H.S., Handog, E. and Kourosh, S.A. (2021) The dark side of skin lightening: an international collaboration and review of a public health issue affecting dermatology. *International Journal of Women's Dermatology*, **7**: 158.
2. Hamann, C.R., Boonchai, W., Wen, L., Sakanashi, E.N., Chu, C.-Y., Hamann, K., Hamann, C.P., Sinniah, K. and Hamann, D. (2014). Spectrometric analysis of mercury content in 549 skin-lightening products: is mercury toxicity a hidden global health hazard? *Journal of the American Academy of Dermatology*, 70: 281-287.
3. Rohman, A. and Wijayanti, E. (2015). Development and validation of atomic absorption spectrometry for the determination of zink and mercury analyzer for determination of mercury in cream cosmetics. *Journal of Food and Pharmaceutical Sciences*, 3: 23-26.
4. Gao, Y., Shi, Z., Zong, Q., Wu, P., Su, J. and Liu, R. (2014). Direct determination of mercury in cosmetic samples by isotope dilution inductively coupled plasma mass spectrometry after dissolution with formic acid. *Analytica Chimica Acta*, 812: 6-11.
5. Zheng, C., Tang, J., Pan, X., Shen, H., Hu, Z., Zhang, J., Wang, L., Wu, P. and Tan, Y. (2025). Development and validation of a high-performance liquid chromatography-inductively coupled plasma mass spectrometry method for the simultaneous determination of arsenic and mercury species in human urine. *Chemosensors*, Multidisciplinary Digital Publishing Institute, 13: 78.
6. Wang, W., Bao, N., Yuan, W., Si, N., Bai, H., Li, H. and Zhang, Q. (2019). Simultaneous determination of lead, arsenic, and mercury in cosmetics using a plastic based disposable electrochemical sensor. *Microchemical Journal*, 148: 240-247.
7. Abels, K., Salvo-Halloran, E.M., White, D., Ali, M., Agarwal, N.R., Leung, V., Ali, M., Sidawi, M., Capretta, A., Brennan, J.D., Nease, J. and Filipe, C.D.M. (2021). Quantitative point-of-care colorimetric assay modeling using a handheld colorimeter. *ACS Omega,* 6: 22439-22446.
8. Joudeh, N. and Linke, D. (2022). Nanoparticle classification, physicochemical properties, characterization, and applications: A comprehensive review for biologists. *Journal of Nanobiotechnology*, 20: 262.
9. Omole, R.K., Torimiro, N., Alayande, S.O. and Ajenifuja, E. (2018). Silver nanoparticles synthesized from bacillus subtilis for detection of deterioration in the post-harvest spoilage of fruit. *Sustainable Chemistry and Pharmacy*, 10: 33-40.
10. Ibrahim, N.H., Taha, G.M., Hagaggi, N.A. and Moghazy, M.A. (2024). Green synthesis of silver nanoparticles and its environmental sensor ability to some heavy metals. *BMC Chemistry*, 18: 7.
11. Salem, H., Samir, E., Salem, H. and Samir, E. (2018). Determination of cefotaxime, cefoperazone, ceftazidime and cefadroxil using surface plasmon resonance band of silver nanoparticles. *Brazilian Journal of Pharmaceutical Sciences*, 54: e17565.
12. Sun, X., Cheng, H., Li, M., Chen, J., Li, D., Liu, B., Jiang, Y., Duan, X. and Hu, J. (2022). Collision electrochemical synthesis of metal nanoparticles using electrons as green reducing agent. *ACS Applied Materials & Interfaces*, 14: 57189-57196.
13. Aldebasi, S., Tar, H., S. Alnafisah, A., Beji, L., Kouki, N., Morlet-Savary, F., Alminderej, F.M., Aroua, L.M. and Lalevée, J. (2023). Photochemical synthesis of noble metal nanoparticles: influence of metal salt concentration on size and distribution. *International Journal of Molecular Sciences*, 24: 14018.
14. Chen, S., Xu, Y., He, X., Su, Y., Yang, J., Chen, W. and Tan, H. (2019). Microemulsion synthesis of nanosized calcium sulfate hemihydrate and its morphology control by different surfactants. *ACS Omega*, 4: 9552-9556.
15. Vu, D.K.N. and Nguyen, D.K.V. (2021). Gamma irradiation-assisted synthesis of silver nanoparticle-embedded graphene oxide-TiO_2 nanotube nanocomposite for organic dye photodegradation. *Journal of Nanomaterials*, 2021: 6679637.
16. Radoń, A. and Łukowiec, D. (2018). Silver Nanoparticles synthesized by UV-irradiation

method using chloramine t as modifier: structure, formation mechanism and catalytic activity. *CrystEngComm*, 20: 7130-7136.
17. Ismillayli, N., Suprapto, S., Santoso, E., Nugraha, R.E., Holilah, H., Bahruji, H., Jalil, A.A., Hermanto, D. and Prasetyoko, D. (2024) Microwave-assisted synthesis of silver nanoparticles as a colorimetric sensor for hydrogen peroxide. *RSC Advances*, **14**: 6815-6822.
18. Odeniyi, M.A., Okumah, V.C., Adebayo-Tayo, B.C. and Odeniyi, O.A. (2020). Green synthesis and cream formulations of silver nanoparticles of *Nauclea latifolia* (African Peach) fruit Extracts and Evaluation of Antimicrobial and Antioxidant Activities. *Sustainable Chemistry and Pharmacy*, 15: 100197.
19. Srikar, S.K., Giri, D.D., Pal, D.B., Mishra, P.K. and Upadhyay, S.N. (2016). Green synthesis of silver nanoparticles: A review. *Green and Sustainable Chemistry*, 6: 34.
20. Zargar, V., Asghari, M. and Dashti, A. (2015). A review on chitin and chitosan polymers: structure, chemistry, solubility, derivatives, and applications. *ChemBioEng Reviews*, 2: 204-226.
21. Zain, N.M., Stapley, A.G.F. and Shama, G. (2014). Green synthesis of silver and copper nanoparticles using ascorbic acid and chitosan for antimicrobial applications. *Carbohydrate Polymers*, 112: 195-202.
22. Borman, P. and Elder, D. (2017) Q2(R1) Validation of analytical procedures. ICH Quality Guidelines, John Wiley & Sons, Ltd, 127-166.
23. Janah, I.M., Roto, R. and Siswanta, D. (2022). Effect of ascorbic acid concentration on the stability of tartrate-capped silver nanoparticles. *Indonesian Journal of Chemistry*, 22: 857-866.
24. Yusniar, Y., Hindryawati, N. and Ruga, R. (2021) Sintesis nanopartikel perak menggunakan reduktor asam askorbat. *Prosiding Seminar Nasional Kimia*, 2021: 187-192.
25. Sankar, R., Rahman, P.K.S.M., Varunkumar, K., Anusha, C., Kalaiarasi, A., Shivashangari, K.S. and Ravikumar, V. (2017). Facile synthesis of *Curcuma longa* tuber powder engineered metal nanoparticles for bioimaging applications. *Journal of Molecular Structure*, 1129: 8-16.
26. Sobczak-Kupiec, A., Malina, D., Wzorek, Z. and Zimowska, M. (2011). Influence of silver nitrate concentration on the properties of silver nanoparticles. *Micro Nano Letters*, **6**: 656-660.
27. Venkatesham, M., Ayodhya, D., Madhusudhan, A., Veera Babu, N. and Veerabhadram, G. (2014) A novel green one-step synthesis of silver nanoparticles using chitosan: Catalytic activity and antimicrobial studies. *Applied Nanoscience*, 4: 113-119.
28. Solomon, S.D., Bahadory, M., Jeyarajasingam, A.V., Rutkowsky, S.A., Boritz, C. and Mulfinger, L. (2007) Synthesis and study of silver nanoparticles. *Journal of Chemical Education*, 84: 322-325.
29. Kumar, V., Singh, D.K., Mohan, S., Bano, D., Gundampati, R.K. and Hasan, S.H. (2017). Synthesis of silver nanoparticle for the selective and sensitive colorimetric detection of mercury (II) Ion. *Journal of Photochemistry and Photobiology B: Biology*, 168: 67-77.
30. Ho, Y.B., Abdullah, N.H., Hamsan, H. and Tan, E.S.S. (2017) Mercury contamination in facial skin lightening creams and its health risks to user. *Regulatory Toxicology and Pharmacology,* 88: 72-76.
31. Peregrino, C.P., Moreno, M.V., Miranda, S.V., Rubio, A.D. and Leal, L.O. (2011). Mercury levels in locally manufactured Mexican skin-lightening creams. *International Journal of Environmental Research and Public Health*, 8: 2516-2523.